Chapter 8

EFFECT OF FIN FLEXIBILITY ON THE OPTIMAL TRAJECTORY

The structure that reinforces the caudal fin of fish is generally comprised by a set of fin rays, that can be bony or cartilaginous and support a softer collagenous membrane (Lauder, 2000; Lingham-Soliar, 2005). Both the fin rays and the membrane are compliant, with the Young's modulus of bony rays being of the order of 1GPa and that of the membrane of 0.3–1 MPa (Lauder and Madden, 2007). Flexibility is a common feature in the propelling surfaces of most animals (Lucas et al., 2014) and results in significant deformations occurring with the propeller motion. The effect of flexibility on the propulsive characteristics of lift-producing caudal fins and wings has been studied extensively, with variable results being reported.

Many of these studies have focused on the simplified problem of heaving and pitching motions of airfoils. An experimental investigation by Prempraneerach et al. (2003) reported an increase of up to 36% in efficiency with a small decrease in thrust for airfoils with chordwise flexibility performing combined heaving and pitching motions. Heathcote et al. (2008) observed an increase in both efficiency and thrust for small values of spanwise flexibility in the heaving motion of a wing of AR=3, while larger compliances resulted in detrimental effects. Simplified theoretical models typically make use of flat plate geometries and inviscid fluid formulations. Katz and Weihs (1978) analyzed the performance of a plate whose leading edge performed a harmonic oscillation, and found increases of up to 20% in efficiency when chordwise flexibility was introduced, with small decreases in thrust. More recent results of a plate in pitching (Alben, 2008) and heaving (Michelin and Llewellyn Smith, 2009) motion found a series of peaks at which the thrust production increased, with regions where the chordwise flexibility produced higher efficiencies. Numerical studies have reached similar conclusions. Liu and Bose (1997) observed a decrease in propulsive efficiency with passive spanwise flexibility, but reported an increase with carefully controlled flexibility, and Zhu (2007) reported an increase in efficiency with chordwise flexibility, while spanwise flexibility was always detrimental when considering motions in a heavy fluid. Overall, these studies have established the benefits of utilizing propellers within specific optimal flexibility ranges. Deviations from these optimal compliance values, however, commonly resulted in reduced

performance.

The effect of compliance on the maneuverability of these fins has received, on the other hand, little attention. Kim and Gharib (2011a) and Kim and Gharib (2011b) investigated the thrust performance of flexible fins for drag-based paddling propulsion, which provides some insight into the behavior of flexible fins performing drag-based maneuvering. They reported a markedly different vortex formation process for an impulsively translating flexible fin compared to that of rigid fins, both flat and curved. These differences resulted in a smaller initial force peak for the flexible fin, which was able, however, to maintain a larger force after this initial peak due to slower vortex development.

These results have highlighted the potential of employing a compliant fin to improve the thrust and propulsive efficiency of a lift-based flapping propeller. Because the maneuvering capabilities of a fin are dependent on rapid, large forces the ability to utilize such a fin for fast turning is yet to be determined. The objective of this chapter is, therefore, to research the effect of fin flexibility in the optimal three-dimensional trajectory that generates a maneuvering side force, with the view of a mechanism that utilizes the same fin for propulsion and maneuvering purposes, such as the one considered here.

8.1 Results

The optimal trajectory, as defined by equation 6.1, followed by a fin of AR=4 and varying flexibility to generate a side force of F_{target} = 17mN was searched using the optimization procedure described in Chapter 6. The fins had a rigid arm and a flexible main surface made of polycarbonate (see figure 6.3b), with thicknesses of h_1 = 0.762 mm, h_2 = 0.508 mm and h_3 = 0.254 mm which constitute flexural rigidities of D_1 = 0.1 Pa m^3, D_2 = 0.03 Pa m^3 and D_3 = 0.004 Pa m^3, respectively. The parameters of the resulting optimal trajectories are presented in table 8.1, together with those obtained for the rigid fin of Chapter 7. The similarity between the trajectories is remarkable, and emphasizes the effectiveness of the identified strategy. The four segments or maneuvers described in detail in Chapter 7 are employed by all four fins. The flexible fins, however, were observed to deform in their motion (figure 8.2), generating differences in the forces produced and their direction. Due to this deformation, the position of the surface of flexible fins cannot be easily obtained at every instant, requiring three-dimensional tracking of the structure, which has not been performed in the current work. The motion of

Parameter	Symbol	Rigid	h=0.76mm	h=0.51mm	h=0.25mm
Type	—	Ellipse	Ellipse	Ellipse	Ellipse
Stroke angle	ϕ	36.0°	38.3°	33.5°	39.6°
Deviation angle	ψ	19.9°	20°	20°	14.6°
Rotation angle	χ	−70°	−70°	−70°	−70°
Rotation phase	β	0	0	0	0.2
Rotation acceleration	K_v	0.2	0	0.2	0.1
Speed-up code	S	2	3	3	0
Speed-up value	γ	1	1	1.1	1.2
Camber	λ	0.4	0.4	0	0.3
Frequency	f	0.19 Hz	0.18Hz	0.2Hz	0.2Hz
Force	$F_{x'}$	17.07mN	17.24mN	17.13mN	17.14mN
Efficiency	η	0.829	0.739	0.700	0.605

Table 8.1: Parameters of optimal trajectories for flexible fins.

these fins disregarding their deformation is very similar to that represented in figure 7.3 for the rigid fin, and has therefore not been included here.

The force diagrams, on the other hand, see significant differences and are represented in figure 8.1. For an approximate correspondence between instantaneous force and fin motion the reader is referred to figure 7.3. In the case of a flexible plate, the normal and tangential vectors vary along the plate's surface and are dependent on its deformation, which is not known a priori. The normal and tangential directions have been defined in this chapter as the normal and tangential directions of a rigid fin with the same rotation values as the flexible fin. Because the deformations are relatively small, this approximation provides a good representation of the directionality of the forces. A clarification should be made, however, about the efficiency. Since the definition of efficiency includes the value of the normal force in the denominator, it does not represent the exact same ratio for rigid and flexible plates. Due to the small deflections the differences are small enough, however, that a reasonable comparison may still be made.

The trajectory obtained for the stiffest of the flexible fins ($h_1 = 0.762$ mm), is almost identical to that obtained for the rigid fin. Although slight variations are present in stroke angle, rotation acceleration and frequency, these are within the
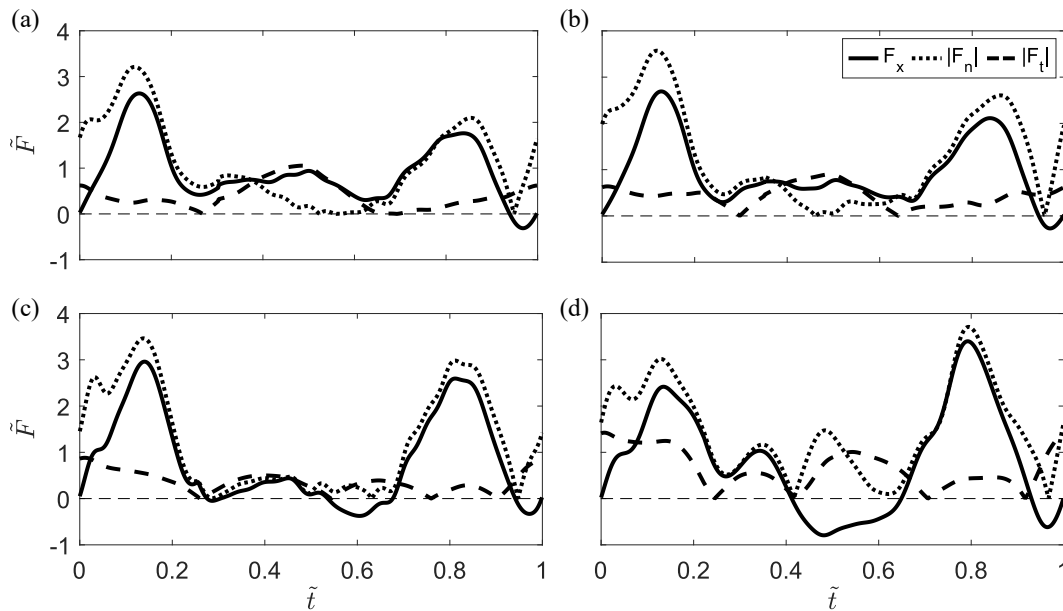
Figure 8.1: Forces generated during the optimal trajectory of the (a) rigid fin and flexible fins of thickness (b)h=0.76mm (c)h=0.51mm and (d) h=0.25mm

convergence criteria established for the optimization (table 6.1). It is interesting to note that, despite moving at a lower frequency and only small variations in stroke angle, the trajectory for the flexible plate has converged to a slightly higher force than that of the rigid plate. Because the target force has been set to $F_{x'} = 17mN$, this does not imply that the rigid plate is not capable of generating such forces, but it does highlight the ability of the flexible plate to produce high enough forces in its motion. The efficiency of the trajectory obtained by the flexible fin, $\eta = 0.74$, is, however, lower than that of the rigid plate $\eta = 0.83$, albeit moderately so. The cause of this reduction in efficiency is visible in the force measurements presented in figure 8.1, where figure 8.1(a) corresponds to the rigid fin and 8.1(b) to the least flexible case. The curve of the $F_{x'}$ force is similar between both cases, with the peak corresponding to segment III of the trajectory being slightly sharper in the flexible fin to compensate for a slightly lower value in segment II. The normal force, on the other hand, sees more significant variations. The flexible fin presents higher normal force values both in section I and III of the trajectory. This implies that the deflection of the plate causes a smaller proportion of the normal force to be in the desired x' direction during these two power motions. Because the averaged $F_{x'}$ force is approximately equal, the flexible fin will require the production of a higher normal force, which results in a lower efficiency.

The optimal trajectory corresponding to the fin of middle flexural rigidity (h_2 = 0.508mm) produces a lower efficiency, $\eta = 0.70$, than that of both rigid and stiffer flexible fins. In this case, however, the decay in efficiency is not produced in segments I and III, with the proportion of the normal force that is directed in the x' direction being similar to that of the rigid plate (figure 8.1c). While most of the normal force at the start of segment II is directed in the x' direction, no surge in tangential force occurs once the normal force decays. This may be due to the deformation of the fin, that generates a curvature on its surface. This curvature modifies the force direction and affects the formation and shedding of vortices, which play an important role in the force generation during this segment. The lack of a tangential force constitutes a detrimental effect on itself, because, as specified in Chapter 7, a tangential force with an x' component has a significant positive impact on the efficiency. In addition to this reduced tangential force, the direction of the small generated forces is detrimental, producing a net force in the negative x' direction at the end of segment II (starting approximately when the fin is located at the major axis of the ellipse) and beginning of segment III. The decrease in both normal and tangential forces in segment II of the trajectory is associated to the increase in the trajectory's frequency. Because the overall force must remain at $17mN$, the forces in the other segments, which are mostly drag-based, must increase. This is achieved by utilizing a higher velocity. There is, in particular, a substantial increase in the peak force produced in segment III, that may be additionally related to release of stored strain energy in the deformed fin. Overall, the efficiency decrease is not sharp, and the fin is capable of generating the required force. If such a degree of flexibility is largely beneficial to the propulsive efficiency of the system, it may constitute a reasonable compromise.

As the rigidity of the fin is decreased, the efficiency drops further, with the most compliant fin presenting an efficiency of $\eta = 0.61$. At this $h_3 = 0.254$ mm, the values of the optimal parameters start to deviate substantially from those of the rigid fin. Although the general strategy remains equal to that of the rigid case, the forces generated are considerably disparate. A second peak in normal force, directed along the x' axis, appears after segment I of the trajectory and may be produced by the release of strain energy accumulated during the power stroke of segment I. Throughout, considerable tangential forces are generated, no doubt due to the higher curvature of the deformed fin, that increases the cross-sectional surface when the fin undergoes tangential motions and modifies the force direction when it undergoes normal motions. An effect similar to that present in the fin of thickness
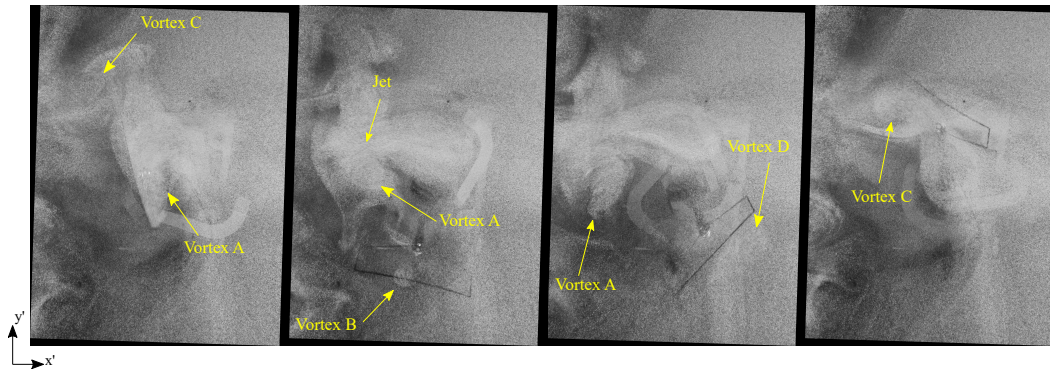
Figure 8.2: Visualization of the fin deflection and flow patterns during the optimal trajectory for a flexible fin of thickness h=0.25mm

$h_2 = 0.508$mm is present, where $F_{x'}$ becomes negative in segment II. The length of this negative interval, as well as the minimum force are largely increased. The peak force generated in segment III increases commensurately, with the average force being maintained at $F_{x'} = 17.14mN$. Although this optimal trajectory is capable of generating the desired force, the use of this higher flexibility generates larger forces in undesired directions, which reduce the efficiency and may pose a complication when performing maneuvering motions. Despite this larger decrease, the efficiency of this trajectory is still significantly higher than that obtained for a rigid plate when its centerpoint motion was limited to a line, evaluated in Chapter 7, further emphasizing the critical importance of employing three-dimensional motions and large rotations when attempting to generate side forces with a flexible fin.

Qualitative flow visualization was performed on the flexible fins, and showed a similar vortex structure to that present in the optimal motion of the rigid fin. The timing of vortex formation and shedding, as well as subsequent vortex dynamics display variations. Images of the visualization for the most flexible fin ($h_3 = 0.254$ mm) are presented in figure 8.2, where the deformation of the fin is also visible. Despite presenting the smallest opposition of all three cases, the deformations of this fin are still modest. The vortices present in these images are similar to those of the rigid case. A leading edge vortex (vortex A) is generated during segment I and is later shed over the fin's trailing edge. A second leading edge vortex (vortex B) is generated at the start of segment II. In this case, however, it detaches close to the fin's leading edge and does not follow a downwards motion. The markedly different behavior of this vortex may be a significant contributor to the detrimental forces generated in segment II of the flexible fin's motion. A third large vortex (vortex D) is

generated during segment III and is shed at the start of the large rotation in segment IV. A final vortex (vortex C) is generated in this rotation and follows an upwards motion after detachment. A similar high-velocity jet is generated and moves in the negative x' direction.

8.2 Conclusions

Flexible fins have been proven in the literature to improve the thrust performance of flapping propellers for specific fin compliance values. The effect of adding a degree of flexibility to the fin on the maneuvering performance of a three-degree of rotation mechanism was investigated. The optimal trajectory for fins of three different flexibilities was obtained, with all three cases being remarkably similar to that of a rigid fin.

The flexible fins were capable of generating the target side force, $F_{x'}$, but did so with lower efficiency than the rigid fin. While the stiffer fins saw a smaller reduction in efficiency, the efficiency decreased as fin flexibility increased. It may, therefore, be possible to find a compromise value of the fin compliance where the propulsive efficiency is benefited from flexibility without largely reducing the maneuvering efficiency. Reductions in the efficiency of the flexible plates are a result of a combination of factors related to the deformation of the plate, including the modification of the force directionality and value, modification of the vortex formation processes and modification of the timing between fluid and fin dynamics.